Research Article | Vol. 25, No. 10 | 15 May 2017 | OPTICS EXPRESS 11622

Optics EXPRESS

Diode-side-pumped Alexandrite slab lasers

M. J. DAMZEN,[1,*] G. M. THOMAS,[1] AND A. MINASSIAN[2]

[1]*Photonics Group, The Blackett Laboratory, Dept. of Physics, Imperial College London, Prince Consort Rd., London SW7 2AZ, UK*
[2]*Unilase Ltd., Unit G02, 1 Filament Walk, London SW18 4GQ, UK*
[*]*m.damzen@imperial.ac.uk*

Abstract: We present the investigation of diode-side-pumping of Alexandrite slab lasers in a range of designs using linear cavity and grazing-incidence bounce cavity configurations. An Alexandrite slab laser cavity with double-pass side pumping produces 23.4 mJ free-running energy at 100 Hz rate with slope efficiency ~40% with respect to absorbed pump energy. In a slab laser with single-bounce geometry output power of 12.2 W is produced, and in a double-bounce configuration 6.5 W multimode and 4.5 W output in TEM_{00} mode is produced. These first results of slab laser and amplifier designs in this paper highlight some of the potential strategies for power and energy scaling of Alexandrite using diode-side-pumped Alexandrite slab architectures with future availability of higher power red diode pumping.

Published by The Optical Society under the terms of the Creative Commons Attribution 4.0 License. Further distribution of this work must maintain attribution to the author(s) and the published article's title, journal citation, and DOI.

OCIS codes: (140.3480) Lasers, diode-pumped; (140.3600) Lasers, tunable.

References and links

1. J. Walling, O. G. Peterson, H. Jenssen, R. Morris, and E. W. O'Dell, "Tunable Alexandrite lasers," IEEE J. Quantum Electron. **16**(12), 1302–1315 (1980).
2. J. W. Kuper, T. Chin, and H. E. Aschoff, "Extended tuning range of Alexandrite at elevated temperatures," in *Proc. Advanced Solid State Lasers* (OSA, 1990), paper CL3.
3. J. Walling, D. F. Heller, H. Samelson, D. J. Harter, J. Pete, and R. C. Morris, "Tunable Alexandrite lasers: development and performance," IEEE J. Quantum Electron. **21**(10), 1568–1581 (1985).
4. R. Scheps, B. M. Gately, J. F. Myers, J. S. Krasinski, and D. F. Heller, "Alexandrite laser pumped by semiconductor lasers," Appl. Phys. Lett. **56**(23), 2288–2290 (1990).
5. R. Scheps, J. F. Myers, T. R. Glesne, and H. B. Serreze, "Monochromatic end-pumped operation of an Alexandrite laser," Opt. Commun. **97**(5-6), 363–366 (1993).
6. E. Beyatli, I. Baali, B. Sumpf, G. Erbert, A. Leitenstorfer, A. Sennaroglu, and U. Demirbas, "Tapered diode-pumped continuous-wave Alexandrite laser," J. Opt. Soc. Am. B **30**(12), 3184–3192 (2013).
7. I. Yorulmaz, E. Beyatli, A. Kurt, A. Sennaroglu, and U. Demirbas, "Efficient and low-threshold Alexandrite laser pumped by a single-mode diode," Opt. Mater. Express **4**(4), 776–789 (2014).
8. X. Peng, A. Marrakchi, J. C. Walling, and D. F. Heller, "Watt-level red and UV output from a CW diode array-pumped tunable Alexandrite laser," *Proc. CLEO* (2005), paper CMAA5.
9. M. Strotkamp, U. Witte, A. Munk, A. Hartung, S. Gausmann, S. Hengesbach, M. Traub, D. Hoffmann, J. Hoeffner, and B. Jungbluth, "Broadly tunable, diode pumped Alexandrite laser," in *Proc. Advanced Solid State Lasers* (OSA, 2013), paper ATu3A.42.
10. A. Teppitaksak, A. Minassian, G. M. Thomas, and M. J. Damzen, "High efficiency >26 W diode end-pumped Alexandrite laser," Opt. Express **22**(13), 16386–16392 (2014).
11. G. M. Thomas, A. Minassian, X. Sheng, and M. J. Damzen, "Diode-pumped Alexandrite lasers in Q-switched and cavity-dumped Q-switched operation," Opt. Express **24**(24), 27212–27224 (2016).
12. A. Munk, B. Jungbluth, M. Strotkamp, S. Gaussmann, D. Hoffmann, R. Poprawe, and J. Hoeffner, "Diode-pumped Alexandrite Ring Laser," in *Proc. Advanced Solid State Lasers* (OSA, 2015), paper ATh2A.46.
13. E. A. Arbabzadah and M. J. Damzen, "Fibre-coupled red diode-pumped Alexandrite TEM_{00} laser with single and double-pass end-pumping," Laser Phys. Lett. **13**(6), 065002 (2016).
14. W. Kerridge-Johns and M. J. Damzen, "Analytical model of tunable Alexandrite lasing under diode end-pumping with experimental comparison," J. Opt. Soc. Am. B **33**(12), 2525–2534 (2016).
15. J. M. Eggleston, T. J. Kane, J. Unternahrer, and R. L. Byer, "Slab-geometry Nd:glass laser performance studies," Opt. Lett. **7**(9), 405–407 (1982).
16. A. Dergachev, J. H. Flint, Y. Isyanova, B. Pati, E. V. Slobodtchikov, K. F. Wall, and P. F. Moulton, "Review of multipass slab laser systems," IEEE J. Sel. Top. Quantum Electron. **13**(3), 647–660 (2007).
17. A. Minassian, B. Thompson, and M. J. Damzen, "Ultrahigh efficiency TEM_{00} diode-side-pumped Nd:YVO_4 laser," Appl. Phys. B **76**(4), 341–343 (2003).

#283519 https://doi.org/10.1364/OE.25.011622
Journal © 2017 Received 22 Dec 2016; revised 1 Feb 2017; accepted 2 Feb 2017; published 10 May 2017

Optics EXPRESS

18. A. Minassian, B. Thompson, and M. J. Damzen, "High-power TEM_{00} grazing-incidence Nd:YVO_4 oscillators in single and multiple bounce configurations," Opt. Commun. **245**(1-6), 295–300 (2005).
19. A. Teppitaksak, G. M. Thomas, and M. J. Damzen, "Investigation of a versatile pulsed laser source based on a diode seed and ultra-high gain bounce geometry amplifiers," Opt. Express **23**(9), 12328–12336 (2015).

1. Introduction

Alexandrite, the common name for the crystal chromium-doped chrysoberyl (Cr^{3+}:$BeAl_2O_4$), has many excellent properties that make it extremely favourable as a solid-state laser material. It is a broadly tunable solid-state laser resulting from a vibronic energy level system and historically is the first tunable laser crystal operating at room temperature. The laser material has been shown to be capable of being tuned from 701 – 858 nm [1,2], although in practice operation is usually over its more central range from ~730 – 800 nm. It is mechanically strong with a fracture limit 5 times greater than Nd:YAG [1]. It has excellent thermal properties including a thermal conductivity (23 W/mK) almost twice as great as Nd:YAG [1]. It is naturally birefringent giving highly polarised output parallel to the crystal *b*-axis and making it mostly immune to depolarisation by stress-induced birefringence. These combined properties together with a high optical damage threshold favours high average power operation with > 100W output demonstrated under lamp-pumping [3].

An important feature of the vibronic crystal Alexandrite is its very broad absorption bands throughout the visible and UV portions of the electromagnetic spectrum with two main peaks centred at 590 nm and 410 nm. The broad absorption spectrum is suitable for lamp-pumping [1–3], but the band with peak centred at 590 nm is sufficiently broad, with strong enough absorption to be suitable for pumping with commercially-available red semiconductor diode lasers (AlGaInP) in the range 630 – 680nm. With lasing near 750 nm, this leads to a small quantum defect. Diode pumping offers the prospect of order-of-magnitude increase in wall-plug efficiency compared to lamp-pumping and also low heat dissipation in the laser crystal. Direct diode-pumping of Alexandrite was first demonstrated by Scheps in the early 1990s [4,5] but at low mW power levels due to the immaturity of red laser diodes. It has been only recently over the last ten years that higher power demonstrations of red-diode end-pumped Alexandrite have been performed, including with single emitter pump [6,7], diode-bar array [8–12], and fibre-delivered diode pumping [13,14].

One of the potential applications of wavelength tunable Alexandrite lasers is for remote sensing based on LIDAR, where for atmospheric sensing high Q-switched pulse energies of multi-ten to hundred mJ are required. Alexandrite has a long upper-state lifetime of 262 μs at room temperature [1] that is favourable for good energy storage in Q-switched operation under diode-pumping. In our previous work [10] we demonstrated the first Q-switched diode-pumped Alexandrite laser producing pulse energy of 0.74 mJ at 1 kHz pulse rate. More recently, we demonstrated Q-switching with up to 3mJ pulse energy [11]. By employing a cavity-dumped Q-switching system, we also demonstrated much shorter pulse duration < 3 ns, independent of repetition rate up to 10 kHz, and 0.5mJ pulse energy at 3 kHz [11].

In all the above publications on diode-pumped Alexandrite [4–14], an end-pumped geometry was used. Whilst this is advantageous for good coupling to the TEM_{00} mode, it is well-known that end-pumping has some inherent limitations, especially at high powers. In particular two main problems are: strong thermally-induced lensing; and the need for high brightness diode pump sources. The recent Q-switched 3 mJ pulse demonstration in diode-pumped Alexandrite [11] also shows the need for considerable further energy scaling if they are to address high energy (~100mJ) applications such as atmospheric LIDAR.

In this paper, we describe our investigations of diode-side-pumped Alexandrite slab lasers in a range of cavity designs. The side-pumped slab geometry has several potential advantages over the end-pumped geometry [15, 16]. These include a large and scalable pump volume for high energy storage. Another advantage is the facility for simple, flexible and scalable pump delivery by pumping via the side face(s) of the slab and the ease of delivering large numbers of low brightness pumps (e.g. bars and stacks) with minimal pump delivery optics. In Section

Optics EXPRESS

2, we present slab laser designs and results using a linear cavity design with both single-pass and double-pass diode-side-pumping. Most efficient operation is provided by a double-pass pumping configuration producing 23.4 mJ of free-running pulse energy at 100 Hz pulse rate and 40% slope efficiency, with respect to absorbed pump energy. In Section 3, we present a second set of designs of Alexandrite slab lasers in grazing-incidence bounce geometries using total internal reflection from the side pump face. The bounce design avoids the hard edge diffraction at the slab side face and provides capacity for averaging of transverse refractive and gain non-uniformity. We show results of 12.2 W continuous-wave output powers using a single bounce slab laser cavity. With a double-bounce slab laser geometry 4.5 W continuous-wave output power is demonstrated in TEM_{00} mode, in a preliminary, as yet unoptimised cavity scheme. The results of slab laser and amplifier designs of this paper highlight some of the potential strategies for power and energy scaling of Alexandrite with future availability of higher power red diode pumping.

2. Side-pumped Alexandrite slab with linear laser cavity

In this section 2, we present operation of diode-side-pumped Alexandrite laser systems with linear laser cavities, and in one case a Z-fold cavity variant. In the later section 3, we present operation of diode-side-pumped Alexandrite in bounce geometry configurations. In both these cavity architectures, two principal diode-side-pump arrangements for the slab were used. The first configuration involves a single pass of diode-pump absorption through the Alexandrite slab, with a pair of pumps from opposite side faces for the linear cavity case. The second configuration uses a double-pass of the diode-pump.

One design issue is the choice of length (L), width (w) and height (h) of the slabs. For the diode side pumping, the crystal width w is a key parameter as the diode radiation is absorbed over this dimension. The width w in combination with the chromium doping concentration of the Alexandrite crystal will determine the fractional absorption efficiency of the pumping radiation. Using Alexandrite slab crystals with two available chromium doping concentrations: 0.16 at.% and 0.22 at.%, our empirical measurement of absorption coefficient or these crystals were ~3.6 cm^{-1} and ~6 cm^{-1}, respectively, at our design red diode pumping wavelength ~636 nm.

For single-pass pumping a slab width w = 4mm was chosen, corresponding to 76% and 90% pump absorption for the two slabs. For double-pass pumping (where the residual transmitted pump is retro-reflected back though the crystal), a slab width w = 2mm was chosen, also leading to the same absorption efficiencies. The single pass pumping has inherent simplicity but even with pumping from both sides of the crystal there is a significant non-uniformity of inversion across the crystal width for good pump absorption, with a minimum inversion in the centre of the crystal. The double-pass pumping improves the uniformity of pumping and, as shown in Section 2.2, the pumping uniformity can be further improved by pumping two regions of the slab with pumps incident from opposite side faces. A further advantage of double-pass pumping is that it concentrates absorbed pump into smaller width intensifying the pumping and hence the gain, which can be particularly advantageous in Alexandrite due to its low stimulated emission cross-section.

2.1 Linear cavity Alexandrite slab laser with single-pass diode-side-pumping

Figure 1(a) shows the Alexandrite slab with single-pass diode side-pumping from two opposite side faces. The laser is a simple plane-plane compact linear cavity. The Alexandrite slab had dimensions: 20 x 4 x 2 mm (L x w x h) and doping concentration 0.16 at.% Cr. The laser end faces are AR coated at the laser wavelength ~755nm. The side faces for diode-pumping are not AR-coated, so the pump wavelength experiences Fresnel losses ~7.3% at normal incidence to these faces (refractive index of Alexandrite = 1.74). The two opposing top and bottom faces are used for conductive cooling to provide temperature control of the crystal and extraction of the deposited heat due to the pumping using a water-cooled

Optics EXPRESS

manifold. The high absorbing and emitting *b*-axis of the crystal was oriented vertically (orthogonal to the top and bottom slab faces).

The diode pumps were a pair of 3-bar stacks operating with wavelength ~636 nm. Unlike standard bars with 10 mm emitter width, the stacks incorporated "mini-bars" with 4.2 mm overall bar emitter width. Each bar was composed of 20 emitters with 40 µm emitter width and 200 µm spacing (20% fill factor). The diode bars had 2.8 mm bar-to-bar spacing pitch in the stack. Each stack could deliver power ~50 W in quasi-CW operation, and with 1 ms pump duration corresponding to ~50 mJ per stack. Cylindrical optics were used to project a line of pumping radiation symmetrically on the two opposite side faces of the laser slab. A single diode vertical cylindrical lens (VCL_D) with focal length 100 mm was used for each of the two pump beams to bring the 3 bars of the stack together symmetrically onto the two opposite side faces of the Alexandrite slab. This formed a narrow focused line of pump radiation with vertical pump size ~200 µm, and Rayleigh length (in air) ~2 mm. The pumping provides a narrow sheet of gain across the slab crystal and approximately covered a length ~15 mm of the slab. The polarisation of the diode pump radiation was vertically polarised (optimised using a half-wave plate) to be parallel to the high absorbing *b*-axis of the crystal. For the 4 mm slab width, with absorption coefficient ~3.6 cm^{-1}, approximately 76% of pump was absorbed in a single–pass, which together with the surface Fresnel loss at the uncoated pump face, meant that approximately only 70% of the power of each incident pump was absorbed.

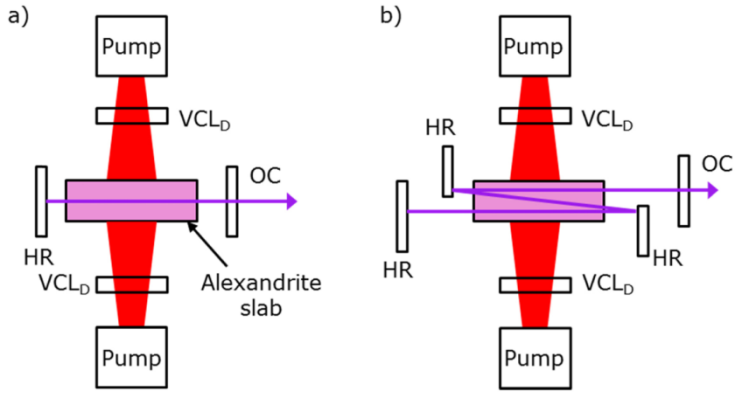

Fig. 1. Diode sided-pumped Alexandrite slab with single-pass pumping with a) a linear laser cavity; and b) a variant 3-pass Z-fold cavity.

The cavity was formed by a plane high reflectivity back mirror (HR) and a plane output coupler (OC) with reflectivity R = 99%. The cavity length ~40 mm was kept as compact as possible to maximise mode coupling to the narrow gain region in the vertical dimension. Since the *b*-axis has by far the highest stimulated emission cross-section, laser emission was strongly vertical in polarisation.

Figure 2 shows the free-running output pulse energy versus total incident pump power from the two diode pumps. The pump duration was 1 ms and pulse rate 100 Hz. Output energy of 4.8 mJ was produced for 98 mJ incident pump power. The slope efficiency was approximately 10%, or 14% with respect to absorbed pump power. The inset of Fig. 2 also shows the spatial profile of the output of the compact linear cavity. The spatial output was image relayed onto a CMOS camera, so the profile shown is an image of the beam at the output coupler. In the vertical direction the beam is fundamental mode, whilst in the horizontal there is considerable structure. The width of the beam is almost precisely 4 mm, the same as the width of the crystal. Two dominant side peaks can be seen in the beam resulting from the higher inversion at the two pump faces. There is evidence of strong diffractive clipping at the side faces of the slab discerned by steep side edges on the beam. Significantly, the central section of the beam has considerably lower intensity, approximately

Optics EXPRESS

third of the intensity at the side peaks. Indeed at low pumping, only the two side regions have sufficient inversion to reach threshold for lasing and appear as two separate unconnected lasing peaks. The strong inversion asymmetry and edge diffraction is undoubtedly contributory to the relatively low efficiency of the system.

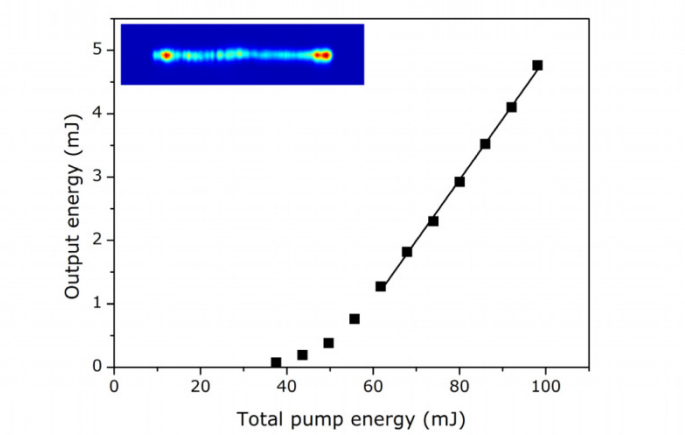

Fig. 2. Free-running output energy versus total incident diode pump energy for single-pass dual-diode side-pumped Alexandrite slab laser with linear compact cavity (Inset: the spatial form of the output beam).

A 3-pass compact Z-fold cavity design shown in Fig. 1(b) was also investigated, utilising an additional pair of cavity mirrors (both HR) to provide the 3-passes in a Z-fold arrangement. The spatial output was found to have a predominantly single top-hat spatial beam structure in the horizontal with size ~1 mm with some modulation. However it was still highly clipped by edge diffraction on both sides by the two slab pump faces. The power efficiency was even lower than the single pass cavity despite the three-passes of gain. It may be possible to improve the efficiency with further cavity design to better mode match to the pump gain region, but we did not pursue this. In the next Section 2.2 double-pass pumping is described and proved to be superior in performance.

2.2 Linear cavity Alexandrite slab laser with double-pass diode-side-pumping

The most efficient version of the linear cavity slab laser configuration was the pump arrangement shown in Fig. 3(a). A photograph of the experimental system is also shown in Fig. 3(b). In this system, double-pass pumping provides a more uniform pump distribution than single pass pumping and the transverse inversion experienced by the laser mode is further flattened by using two separate double-pass pump regions with pumping for each region incident from opposite sides.

The crystal was an Alexandrite slab with length 30 mm, width 2 mm and height 2 mm and nominally 0.22at.% chromium doping. This slab has half the width of the one used for single-pass pumping since absorption is over two passes and this also provides a higher average inversion density by a factor of two. This is advantageous for good laser efficiency, especially in a low gain material as Alexandrite. As with the other slab, the laser end faces were AR coated for the laser wavelength, but the side pump faces were uncoated.

The diode pumping was with the same pair of 3-bar diode stack modules incident from opposite side faces and pumping separate adjacent regions along the length of the slab. Vertical cylindrical lenses (VCL_D, f = 50 mm) were used to focus the pump to a line focus (with vertical height ~100 μm) and horizontal cylindrical lenses (HCL_D) were also used to confine the pumps to their separate lateral regions. The retro-reflection for the double-pass pumping was achieved with a cylindrical curved HR_{RR} diode mirror placed at a distance equal

Optics EXPRESS

to its curvature away from the crystal to vertically re-image the 3 bar stack back together again into the crystal. Another HCL_{RR} was placed in each double-pass pump path to maintain the lateral pump size. The fluorescence from the two separate adjacent pump regions is observable in the two glowing segments of the slab in Fig. 3(b).

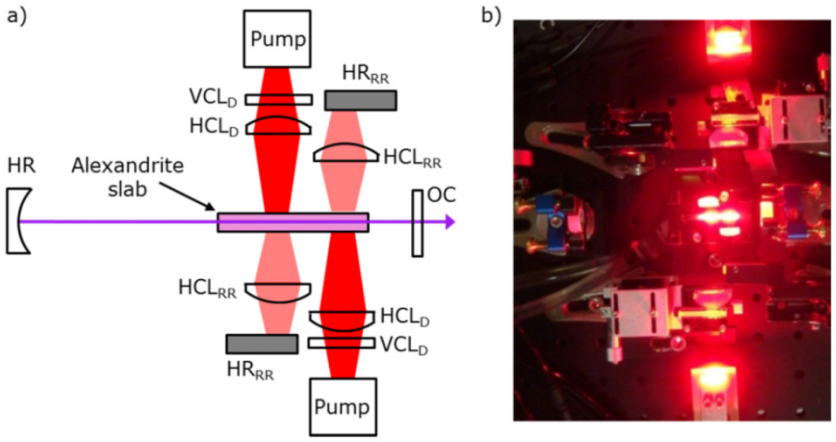

Fig. 3. a) Schematic and b) photograph of dual-sided double-pass diode-pumped Alexandrite slab laser system: the Alexandrite slab can be seen near the centre of the photograph with strong fluorescence visible from the two separate pump regions.

The laser cavity used a plane output coupler and curved HR back mirror with radius of curvature of 100 mm. Maximum efficiency was obtained when the cavity length was approximately the radius of curvature to provide good spatial mode match to the narrow vertical pump distribution. Figure 4 shows the output energy in free-running mode against total diode pump energy incident on the slab amplifier crystal. Three output coupler reflectivities were investigated and displayed in Fig. 4: R = 99.5% (magenta diamonds); R = 99% (open black squares); and R = 98% (red circles). The pump had 1 ms duration and 50 Hz pulse repetition rate.

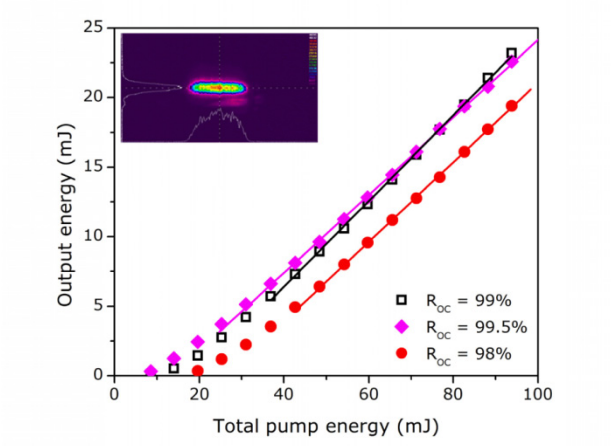

Fig. 4. Double-pass diode-pumped Alexandrite slab laser output energy versus total incident diode pump energy, for output couplers with reflectivity: R = 99.5% (magenta diamonds); R = 99% (open black squares); and R = 98% (red circles). Inset: output spatial beam profile.

The R = 99% output coupler had the highest power 23.2 mJ (with 94 mJ pump energy) and highest slope efficiency (η_s) of 31.2% with respect to incident energy. It is estimated from

Optics EXPRESS

the transmission of the crystal and surface losses of the uncoated pump faces that the double-pass absorption efficiency of the crystal (absorbed pump / incident pump) η_{abs} ~80%. This gives a slope efficiency with respect to the absorbed pump energy $\eta_{s,abs}$ ~40%. The spatial profile of the output laser mode is shown in the inset of Fig. 4. The beam was fundamental mode in the vertical direction but multimode in the horizontal direction, due to the large aspect ratio of the slab gain dimensions in the horizontal (~2 mm) compared to the vertical (~0.1 mm).

Using the 99% reflectivity output coupler, the pulse repetition rate was varied by factors of two, from 25 Hz to 50 Hz and to 100 Hz. The pulse energy in each case was measured as function of incident pump energy as shown in Fig. 5. The pulse energy is almost independent of pulse repetition rate and showed no sign of onset of detrimental thermal effects. Indeed the pulse energy is slightly increasing with repetition rate and may be due to the increasing temperature of the crystal. This is favourable in Alexandrite due to providing higher effective stimulated emission cross-section [1]. The pulse energy at 100 Hz is 23.4 mJ with a slope efficiency of 31.6% (~40% with respect to absorbed pump) and corresponding to a multi-Watt average power of 2.34 W.

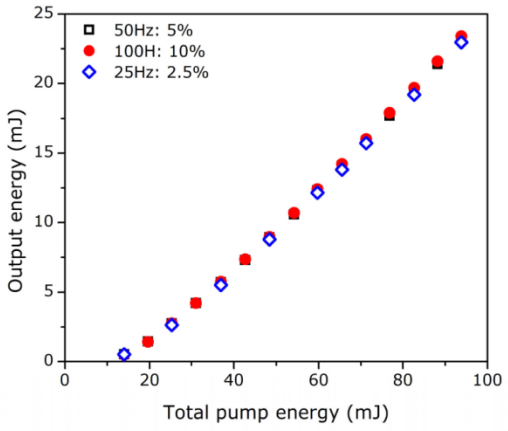

Fig. 5. Alexandrite laser free-running output energy versus total incident diode pump energy at different repetition rates: 25 Hz, 50 Hz and 100 Hz, for 1 ms pump duration. Corresponding pump percentage duty cycles are shown. Output coupler: R = 99%.

The Alexandrite slab laser cavity shown in Fig. 3 was also pumped by the diode stacks operated in continuous wave mode. The corresponding continuous wave output power of the Alexandrite slab laser is shown in Fig. 6 with respect to absorbed pump power (80% of incident power). Output power 6.4 W was achieved with 51.7 W absorbed pump power, with slope efficiency ~20%. The lower slope efficiency compared to the pulsed diode-pumping (1 ms, 100Hz, 10% duty cycle) is thought to be due to the higher thermal lensing. Further cavity design accounting for the stronger thermal lensing should be possible to increase the efficiency of this system.

The diode-side-pumped Alexandrite slab laser in Fig. 3 was modified to attempt to create a TEM_{00} laser design employing cylindrical optics in the cavity to match the TEM_{00} to the highly asymmetric gain profile (width ~2 mm; height ~0.1 mm). The modified cavity consisted of a plane HR back mirror and a plane output coupler mirror, with the Alexandrite slab placed in the centre of the cavity. A pair of vertical cylindrical lenses (VCL, f = 70 mm) was used, positioned symmetrically near the cavity mirrors and close to their focal length from the gain region, to vertically match the TEM_{00} mode to the small vertical dimension of the gain medium. A horizontal cylindrical lens (HCL, f = 200 mm) was positioned near one side of the laser crystal to form a large horizontal mode size in the gain medium (and smaller

Optics EXPRESS

spot sizes at the cavity mirrors). Free-running output energy ~2 mJ was achieved with 40 mJ pulsed pump energy, 1 ms pump duration and 50 Hz pulse repetition rate.

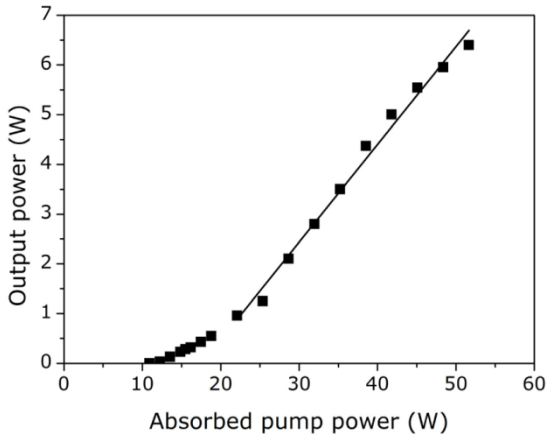

Fig. 6. Continuous-wave operation of Alexandrite slab laser with respect to absorbed pump power.

The M^2 spatial quality of the beam was determined by measuring the beam size as function of propagation distance through a focus formed by a lens (according to the ISO standard method), as depicted in Fig. 7 showing the laser mode size as function of propagation distance through a focus. The M^2 in the horizontal direction was 1.15 and in the vertical direction 1.37 showing that the laser mode is TEM_{00} and near diffraction limited. The energy of the TEM_{00} laser output is significantly less than in the multimode cavity design. This is partially expected because the TEM_{00} mode overlap with the gain will be less than the multimode beam not extracting well at the pump faces of the slab. It was also noticed that during alignment the TEM_{00} laser cavity could spontaneously self-Q-switch, as observed by a giant spike using a photodetector and oscilloscope system. The Q-switching was thought to be caused by cavity perturbation when the laser was being adjusted during alignment whilst in free-running mode.

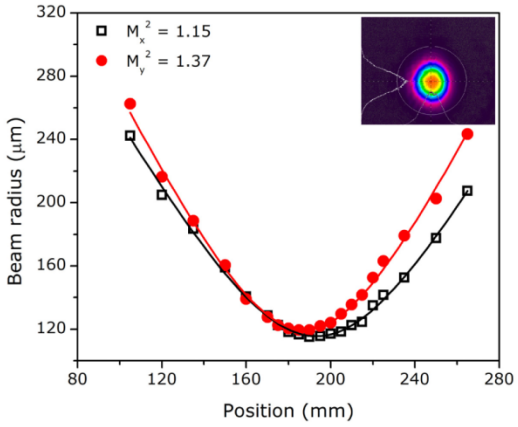

Fig. 7. Spatial beam size propagation through focus to determine M^2 beam quality parameters of the TEM_{00} Alexandrite slab laser design. Beam profile of the spatial output beam also shown.

Optics EXPRESS

3. Diode-side-pumped Alexandrite slab bounce lasers

In the diode-side-pumped Alexandrite slab with transverse linear cavity described in Section 2, there is an issue of diffraction losses and spatial clipping at the hard side edges of the slab. If high efficiency inversion extraction is required these side edge regions of the slab should not be avoided as the pumping is most intense at the pump face. In this Section, we describe investigation of alternative laser geometry for side-pumped slab amplifiers using a grazing-incidence design, commonly known as the bounce geometry [17–19]. In the bounce geometry the laser mode undergoes total internal reflection at a shallow (grazing-incidence) angle, θ_B, at the pump face as shown schematically in Fig. 8. Investigation of this configuration in Alexandrite is described in Section 3.1. For fuller volume extraction a double-bounce design, as shown in below, is also investigated and described in Section 3.2.

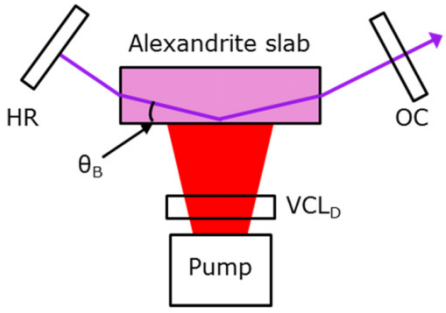

Fig. 8. Schematic diagram of an Alexandrite slab laser using a bounce design where the laser mode undergoes total internal reflection at the side pump face of the slab crystal, at angle θ_B.

3.1 The single-bounce Alexandrite slab laser

The Alexandrite slab laser geometry with single bounce is shown schematically in Fig. 8. The investigated Alexandrite slab in this study had nominal dimensions: 20 x 4 x 2 mm (L x w x h) and doping 0.235% Cr. The laser end faces were AR coated for the laser wavelength but side faces were uncoated. The slab was pumped at one of its uncoated side faces. Instead of the 3-bar stack previously used the pump module in this case was a higher brightness module with 7 mini-bars free-space stacked with a bar-to-bar spacing of 0.8mm and operating at ~638 nm nominal wavelength. The diode module output radiation was focused with a single vertical cylindrical lens (VCL_D) with focal length of 80 mm, giving a vertical pump height FWHM ~120 μm (or Gaussian radius size ~100 μm) at the crystal. The laser path formed a single grazing-incidence with 9° internal bounce angle (θ_B) to the pump face. The cavity back mirror was plane with high reflectivity (HR) at 755 nm, and the output coupling (OC) mirror was plane with different reflectivity R_{OC}. The cavity length was ~34 mm to form a compact symmetric cavity configuration. The crystal absorption coefficient was measured as 5.6 cm^{-1}, corresponding to an absorption depth ~1.8 mm for pump wavelength ~638 nm (diode cooling water temperature = 16°C). The absorbed pump power was ~83% of the incident power lower due to the combination of 7.3% Fresnel reflection loss at the uncoated pump face and the residual unabsorbed pump ~10%. The Alexandrite bounce laser design was run in both pulsed and CW diode pumping modes.

The results of the free-running output pulse energy for pulsed diode-pumped bounce geometry laser are shown in Fig. 9, with pump pulse duration of 1 ms and pulse repetition rate 100 Hz (10% duty cycle). Operation was investigated with three output coupler reflectivities: R = 99%, 98% and 97%. Maximum free-running output energy of 10.8 mJ was achieved for 62 mJ absorbed pump energy with the 98% reflectivity output coupler. The laser slope efficiency increased with decreasing mirror reflectivity over the range used: 18% (R_{OC} = 99%); 23% (R_{OC} = 98%); 25% (R_{OC} = 97%).

Optics EXPRESS

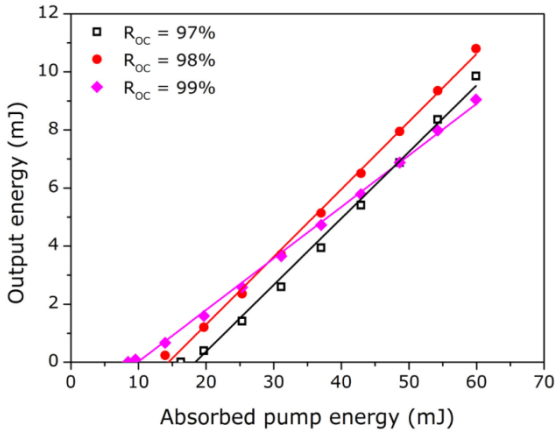

Fig. 9. Output pulse energy in free-running mode of Alexandrite slab bounce laser with pulsed diode pumping (1 ms; 100 Hz) for a range of output coupler reflectivities.

The Alexandrite slab bounce laser cavity was also run with CW diode pumping. The laser output power as function of diode pump power is shown in Fig. 10 for the same three output coupling reflectivities: R = 99%, 98%, and 97% (diode water temperature 16°C). The highest output achieved was again with the 98% mirror. Output power was 11 W (at ~755 nm) for 56 W absorbed pump power. This corresponds to an optical-to-optical conversion of 20% and slope efficiency is ~33%.

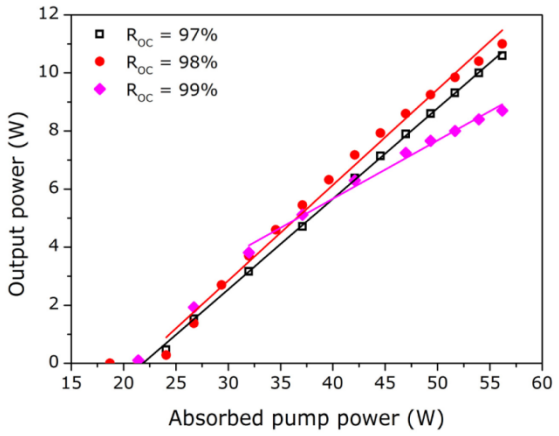

Fig. 10. Output power of CW Alexandrite slab bounce laser for different output coupler reflectivities at diode water temperature 16°C.

The slab bounce laser output efficiency was found to increase with decreasing diode water temperature. To understand this behaviour, the laser output power is plotted as a function of diode pump water temperature with the R = 98% output coupler is shown in Fig. 11. The laser increases in power monotonically with lowered diode temperature, rising from 8.5 W at 25°C to 12.2 W at 12°C. The pump wavelength, also shown in Fig. 11, is seen to tune to shorter wavelength with decreasing temperature, shifting from 640.3 nm at 25°C down to 637.7 nm at 12°C. The efficiency increase can be explained by the decreasing absorption depth as the pump tunes to shorter wavelengths due to the form of the absorption spectrum of Alexandrite. This leads to increased inversion density at the pump face and enhanced extraction efficiency of this region accessible to the laser mode in the bounce geometry. A similar temperature-dependent effect is seen with the pulsed diode pumping case.

Optics EXPRESS

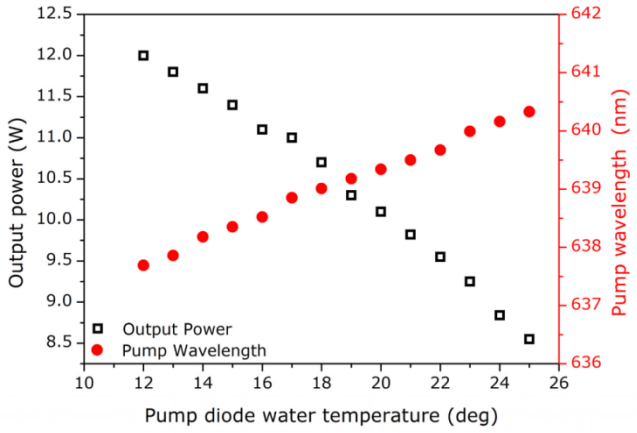

Fig. 11. Output power of Alexandrite slab bounce laser as function of diode water temperature. Variation of pump wavelength is also shown in red. Output coupler R = 98%.

At 12°C diode water temperature for the R = 98% output coupler achieving the highest output power of 12.2 W, the laser slope efficiency was measured in that case to increase to 37%. Figure 12 shows the spectral output for this case at the output power of 12.2W. The peak laser wavelength was 755.3 nm and lasing bandwidth (FWHM) was 1.6 nm.

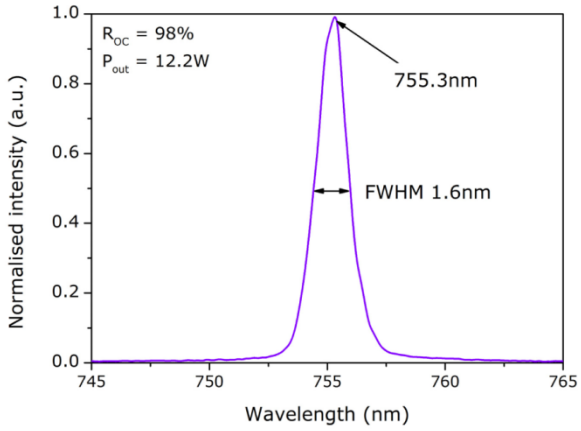

Fig. 12. Lasing spectrum for the Alexandrite bounce laser with R = 98% output coupler, at a diode water temperature of 12°C

It is noted that in addition to the main laser output, the laser mode experiences reflection losses at the two slab crystal faces. This is indicated in the modified schematic diagram in Fig. 13 showing the intracavity surface reflected powers (P_2 and P_3) from the two laser end faces. For the R = 98% output coupler with main output power P_1 = 12.2 W, there was measured > 2 W additional combined lost power ($P_1 + P_2$) from these two end faces. The loss is due to the oblique angle of incidence (16°) of the laser mode in the bounce geometry to the slab end faces when the AR-coatings for these faces are specified for normal incidence. If the coatings are better optimised for this incidence angle, further power efficiency should be possible. If these losses are eliminated the combined total output power ~14.2 W would be projected to be equivalent to a slope efficiency 43%.

Optics EXPRESS

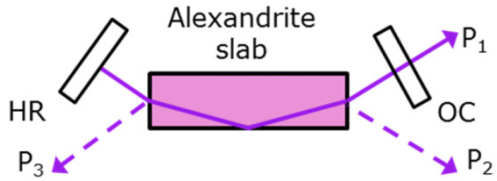

Fig. 13. Modified schematic of the single bounce Alexandrite slab laser, indicating intracavity power losses (P_2 and P_3) at the laser faces.

3.2 Double-bounce Alexandrite slab laser

It is clear from the above that the absorption depth is one of the critical requirements for obtaining good efficiency of the bounce geometry. With a large absorption depth a significant fraction of the pump near the opposite side of the pump face is not accessible to the laser mode and does not get extracted. Operating at much colder diode temperatures to further wavelength shift the diode pump and decrease the absorption depth is not acceptable due to condensation problems for the pump diode. An alternative approach would be to operate with higher doped Alexandrite slab crystals but these are less commonly available. The next geometry explores a possible route for greater volume extraction to be accomplished by utilising a double-bounce geometry.

A schematic diagram of the compact double-bounce geometry laser is shown in Fig. 14(a) and a photo of experimental system in Fig. 14(b). The laser mode makes a total internal reflection (bounce) from both the pump and the opposite side faces on consecutive forward and backward passes through the slab amplifier. The two passes from opposite pump faces have the potential to allow larger mode volume extraction than with a single bounce. The double-bounce geometry has the added potential of increasing the gain of the laser by effectively doubling the gain length via the two passes.

In the experimental implementation of the double-bounce laser configuration a compact cavity (cavity length ~60 mm) was used. The alignment of the laser mode through the two crystal passes was controlled in by a pair of HR mirrors on one side of the Alexandrite crystal. The pump is the tailored 7-bar diode module used in the single bounce slab laser. In this double-bounce configuration, a slab crystal with narrow width of w = 2mm was used (with length L = 15 mm and height h = 2 mm). The crystal doping was nominally 0.22 at.% and had effective absorption coefficient of 6.1 cm^{-1} for the pump radiation with the single pass absorption of the pump measured to be 70%. To enhance the absorption efficiency and improve the pump uniformity, a high reflectivity mirror (HR_{RR}) for the pump was placed in close proximity to the rear side face of the slab and used to retroreflect and double-pass the pump through the slab. This resulted in double pass absorption ~90% through the crystal. Since the pump faces are not AR-coated, there is an additional 7.3% reflection from the input pump surface. As a result, the absorbed pump power is at best ~83% of the incident pump power.

Focusing of the pump was with a single vertical cylindrical lens (VCL_D, f = 150mm) to give a vertical focal diameter ~200 μm (FWHM). At this pump focus, the vertical dimension of the beam had a Rayleigh length (in air) ~5.5 mm, which sufficently exceeds the double-pass absorption length (4 mm) to consider the pump quasi-collimated across the crystal. A bounce angle ~8° is used on both side faces to form a symmetric ‘diamond-shaped’ double-bounce arrangement for this slab dimension (external angle is ~14°). The output coupler mirror had reflectivity of R = 95%. In the photo in Fig. 14(b), it is possible to observe the diamond shaped beam path in the crystal from the change in fluorescence from the extracted path.

Optics EXPRESS

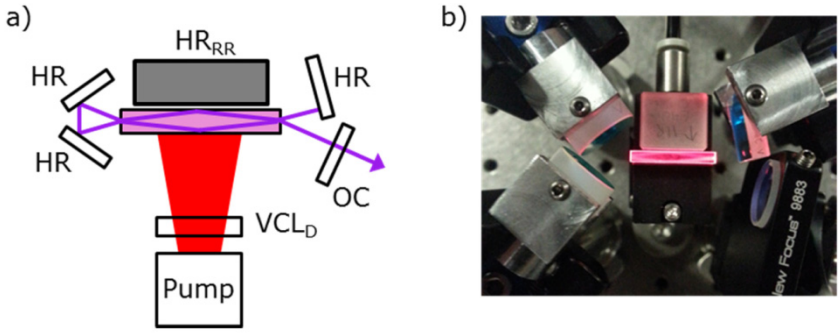

Fig. 14. Side-pumped Alexandrite slab laser in double-bounce geometry: a) schematic of the double-bounce design; b) photograph of experimental system for compact cavity arrangement.

The variation of output power with pump power of this geometry is shown in Fig. 15. An output power of 6.5 W was generated at absorbed pump power 57 W. The optical efficiency is low mainly due to the high threshold and operation close to this threshold. The laser slope efficiency is 32%, indicating reasonably high efficiency can be obtained. The inset of Fig. 15 shows the spatial profile of the output from the compact double-bounce laser. The profile is in fundamental mode in the vertical but the horizontal is multi-mode.

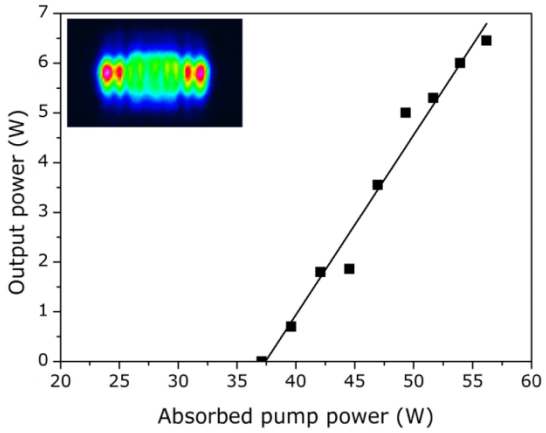

Fig. 15. Output power versus absorbed pump power of diode-pumped Alexandrite slab laser in compact double bounce geometry cavity configuration. Inset: spatial profile of the output.

To obtain TEM_{00} mode operation, Fig. 16 shows schematic of the double-bounce laser designed with an extended output coupler arm. The overall cavity length was ~160 mm. The distance of the output mirror (R = 95%) to the centre of the slab crystal was ~110 mm. A vertical cylindrical lens (VCL) with focal length f = 150 mm was positioned near the output coupler (~150 mm from back mirror) to provide a better overlap with the narrow vertical pump region.

The output power as a function of absorbed pump power of this extended double-bounce laser implementation is shown in Fig. 17. It shows quasi-linear increase in output power with increasing pump power. The threshold pump power is high and similar to the case of the compact cavity configuration. The slope efficiency ~43% is even higher than the compact cavity. The reason for the improved performance may be due to a better spatial mode matching with the gain region by using the intra-cavity cylindrical lens. This high efficiency is promising, since the cavity design is as yet unoptimised (e.g. bounce angle, cavity arm lengths).

Optics EXPRESS

It is worth commenting that there is considerable intra-cavity loss due to the AR coating reflection losses at the multiple 8-passes of the slab end face surfaces at non-zero angle of incidence (twice as many as in the single bounce geometry). This led us to choose the higher output coupling mirror R = 95%, compared to the optimal choice used in the single bounce R = 98%. The higher output coupling helps to maintain the slope efficiency but together with the high AR slab face losses leads to a very high threshold and poorer overall optical-to-optical efficiency since operation is not much above threshold pumping (less than twice threshold pumping).

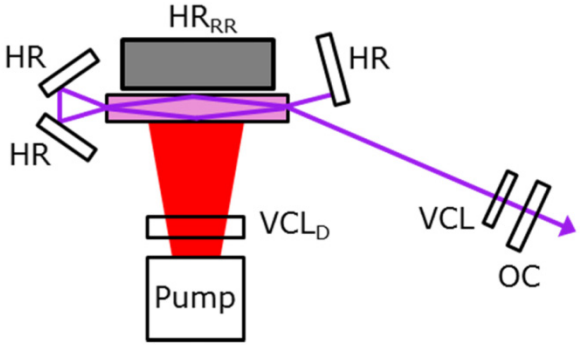

Fig. 16. Side-pumped Alexandrite laser in double-bounce geometry cavity configuration, with extended output arm and vertical cylindrical lens (VCL) for TEM_{00} mode matching to gain region.

The spatial quality in the extended double bounce laser is TEM_{00}, and a beam spatial capture is shown in the inset of Fig. 17. The laser becomes unstable (in the horizontal direction) at output power above ~4.5 W, as noted by the roll-over in power at higher pumping. The design of the cavity should be able to be improved for higher power TEM_{00}, as part of ongoing work, with better mode size optimisation and cavity design and particularly with minimisation of AR end-face intracavity reflection losses. The use of dual-side-pumping with two separate pump beams could also be beneficial for power scaling, as the non-uniform pump distribution does not have the same problems as with edge diffraction losses in the linear cavity schemes.

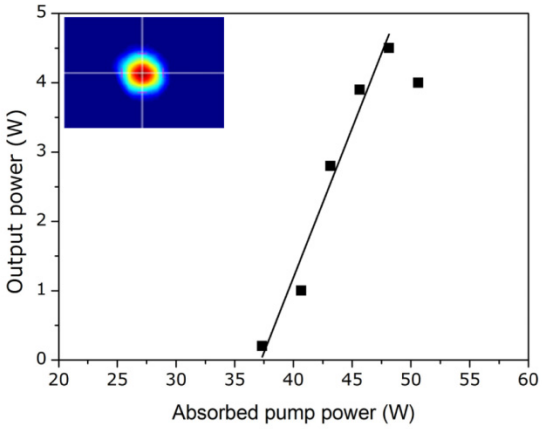

Fig. 17. Output power versus pump power of diode-pumped Alexandrite slab laser in extended double bounce geometry cavity configuration. Spatial TEM_{00} output shown in inset.

Optics EXPRESS

4. Conclusions

Diode-side-pumped Alexandrite slab lasers in linear and bounce geometry laser designs have been demonstrated for the first time. It offers many potential advantages over the end-pumped design, principally the potential for power and energy scaling by using a larger (and scalable) gain volume, and ease of coupling multiple low brightness diode modules to the side pumping faces.

An Alexandrite slab laser with linear cavity design and double-pass side pumping produced 23.4 mJ free-running energy at 100 Hz rate and slope efficiency ~40% with respect to absorbed pump energy. In continuous wave mode, the cavity produced 6.4 W output power.

In a compact CW diode pumped single bounce laser 12.2 W power was generated with a laser slope efficiency of 37%. It was observed that the laser efficiency increased with higher diode absorption coefficient produced by tuning diode to shorter wavelength. In a double-bounce geometry, using total internal reflection from the two side faces, 6.5 W output power was generated in a compact cavity with multimode spatial output and 4.5 W power produced in an extended cavity configuration producing TEM_{00} mode with slope efficiency of 43%. The power and efficiency of the single and double bounce geometry can be further improved by minimising the intra-cavity loss from surface reflections from the laser end faces due to the oblique angle of incidence (AR-coatings were optimised for normal incidence in our experimental system). In the single bounce case elimination of these measured losses is predicted to increase the slope efficiency from 37% to 43% for the single bounce design.

These first diode-side-pumped Alexandrite slab laser demonstrations should be viewed in many cases as preliminary, with the prospect for further optimisation in efficiency and spatial performance. They point to the useful potential that the slab geometry offers for scalable power and pulse energy using higher power arrays of diode-pumping and Q-switched operation. The Alexandrite side-pumped slab therefore looks attractive as an alternative to end-pumping [11], although more work is required in cavity design for high power TEM_{00} operation and wavelength tuning. The diode-side-pumped slab also offers the future prospect of development of high energy amplifiers for Alexandrite oscillator pulses or other lasers (e.g. Ti:sapphire) that operate within its wavelength band.

Funding

We gratefully acknowledge financial support for this work from the European Space Agency (ESA) under contract 4000107239/12/NL/PA.

Acknowledgments

The authors acknowledge valued input from E. Armandillo and C. M. Jost at ESA ESTEC. The authors also acknowledge S. Johnson and M. Kehoe of the Optics Mechanical Workshop at Imperial College London.

155.198.12.188 {ts '2017-06-13 10:38:41'}